# Identification of Ligand Binding Sites on Integrin α4β1 through Chemical Cross-Linking

Ling Ling Chen, Roy R. Lobb, Julio H. Cuervo, Ko-chung Lin, Steven P. Adams, and R. Blake Pepinsky*

*Biogen Inc., 14 Cambridge Center, Cambridge, Massachusetts 02142*

*Received February 6, 1998; Revised Manuscript Received March 26, 1998*

ABSTRACT: We have used chemical cross-linking to identify sequences in integrin α4β1 that are involved in its interactions with ligands. A recently described leucine-aspartic acid-valine (LDV)-based small molecule inhibitor of α4β1 (BIO-1494), that contained a single reactive amino group for targeting the cross-linking, was used for these studies. The specificity of the interaction was defined by (i) the ability to block the interaction with a competitive inhibitor lacking the reactive group, (ii) the absolute requirement of divalent cations for cross-linking, and (iii) the lack of cross-linking to the functionally related integrin α4β7. With ANB-NOS as the cross-linker, only the β1 chain was labeled with BIO-1494, while with the more flexible cross-linker DSS both the α4 and β1 chains were modified. Similar results were obtained when cross-linking was performed on K562 cells expressing α4β1 but not on K562 cells expressing α2β1. The site of cross-linking on the β1 chain was localized by CNBr peptide mapping within residues 130−146, a region that contains the putative metal binding site DXSXS and for which analogous data had been generated with RGD binding to integrin αIIbβ3. The striking similarity between the data we generated for an LDV ligand and published data for the RGD family supports the notion of a common ligand binding pocket formed by both integrin chains. The cross-linking strategy developed here should serve as a useful tool for studying α4β1 function.

Integrin α4β1 (VLA4, very late antigen-4; CD49d/29) is found on the surface of various leukocyte subtypes and interacts with vascular cell adhesion molecule-1 (VCAM-1) and with the alternately spliced CS1 region of fibronectin (*1*−*3*; see *4*, *5* for reviews). These interactions regulate leukocyte migration into tissues during inflammatory responses and normal lymphocyte trafficking (*4*, *5*). While expression of α4β1 is constitutive, its interaction with ligands is strongly enhanced in an activated state, that can be induced by various stimuli including antigen, anti-TCR mAbs, phorbol esters, the divalent cation manganese, and certain β1-specific antibodies (*6*−*8*). Like other integrins, α4β1 function also includes a signal transduction component (*9*−*11*). The mechanisms underlying its activation and the resulting signal transduction events are areas of intensive research (*9*, *11*−*13*).

Integrin α4β1 is a noncovalently associated heterodimeric complex composed of an α4 (molecular mass 155 kDa) and a β1 (molecular mass 150 kDa) chain. The α4 chain exists both in an intact form and as a proteolytically cleaved form composed of 80 and 70 kDa fragments that remain noncovalently associated (*14*−*16*). The ratio of intact to processed form is highly variable from cell type to cell type, but both forms are functional. The entire α4β1 complex can be isolated in a functional state by affinity chromatography using anti-β1 antibodies with detergent-treated cells (*17*). However, rigorous biochemical analysis of α4β1 has been hampered by the paucity of the protein from both natural and recombinant sources. Both the α and β chains are required for integrin function. Critical regions on both chains have been defined with monoclonal antibodies that affect function and through site-directed mutagenesis (*18*−*23*). Further relevant information can be inferred from the striking similarity between the sequence and structure of other integrins (*20*, *24*−*26*).

Previously, ligand binding sites on integrin αIIbβ3 were investigated by cross-linking an RGD-containing peptide substrate to the purified integrin and then using peptide mapping and sequence analysis to identify specific αIIbβ3 peptides in contact with the RGD (*27*). In this manner, Lys-125 from the β chain was found to be in the substrate binding pocket. The same region of β3 was later identified by phage display technology (*25*). This region in the β3 sequence is immediately adjacent to the DXSXS "MIDAS" motif conserved in all integrins and presumed to be involved in metal binding (*20*, *26*, *28*). Similarly, a 20 amino acid region in the α chain of αIIbβ3 in close proximity to the bound RGD ligand was also defined by cross-linking (*29*). The cross-linking data for αIIbβ3 suggest that both chains make up the ligand binding site. To date, there are no direct biochemical data on ligand binding sites in α4β1.

The interactions between α4β1 and its ligands are low affinity (*30*−*32*). Like other adhesion molecules, high avidity interactions presumably result from multivalent interactions (*33*, *34*). Studies with dimeric forms of VCAM support this notion (*35*). This low affinity/high avidity interaction between ligands and their receptors presumably plays an important role in how the adhesion molecules can function. Key residues in VCAM-1 (QIDSP) and CS1

* To whom correspondence should be addressed. Telephone: (617) 679−3310. FAX: (617) 679-2616.

S0006-2960(98)00311-0 CCC: $15.00 
Published on Web 05/27/1998

(EILDVP) that are necessary for their interactions with α4β1 have been defined by molecular and biochemical techniques (*30*, *36*). Recently published crystal structures for the integrin binding region of VCAM-1 revealed that this sequence forms a loop that sticks out from the surface of the molecule (*36*, *37*). While there are no analogous structural data for the CS1 region, the homology between the functional VCAM-1 and CS1 sequences suggests that it will display a similar structure. Many groups have used these sequences as starting points to develop small molecule inhibitors that can block the interaction between α4β1 and its ligands (*38*−*40*). By using a novel capped peptide strategy, we have generated a series of subnanomolar inhibitors selective for α4β1, typified by the compound 4-[(*N*′-2-methylphenyl)ureido]phenylacetyl-LDVP (BIO-1211) (K. C. Lin, R. R. Lobb, and S. P. Adams, unpublished experiments). In this study, we have used a BIO-1211 analogue that could be modified with cross-linking reagents without perturbing function to biochemically investigate the specificity of the BIO-1211 type inhibitor. The binding sites were then localized by peptide mapping. The striking similarity between the data we generated with α4β1, described below, and previously published data for β3 integrins (*25*, *27*) suggests the presence of a highly conserved ligand binding pocket that may be common to all integrins.

## EXPERIMENTAL PROCEDURES

*Purification of α4β1.* The α4- and α2-transfected K562 cell lines were a gift of Dr. Martin Hemler (Dana-Farber Cancer Institute, Boston, MA). An enriched population of the α4-K562 cells that exhibited high levels of α4β1 expression, on average 250 000 copies per cell, was obtained by FACS sorting, and this subclone was used for all subsequent work. The cells were grown at 37 °C in a 10 L bioreactor in RPMI-1640 medium supplemented with 10% fetal bovine serum, 1 mg/mL G418, 10 μg/mL gentamicin sulfate, and 50 μg/mL streptomycin. Cells were collected by centrifugation and lysed in 1% Nonidet P40, 25 mM Tris-HCl, pH 7.4, 1 mM $CaCl_2$, 1 mM $MgCl_2$, 1 mM $MnCl_2$, 2% BSA, 1 mM phenylmethanesulfonyl fluoride at $1 \times 10^8$ cells/mL of lysis buffer. The lysates were clarified by centrifugation and stored at −70 °C for subsequent use. Fifteen milliliters of the α4-K562 cell lysate was incubated for 2 h at 4 °C with 0.5 mL of B5G10-Sepharose 4B that had been conjugated with antibody at 5 mg/mL resin. The resin was collected in a column, and washed with 2 column volumes of lysis buffer without BSA and then with 10 volumes of 0.1% Triton X-100, 25 mM Tris-HCl, pH 7.4, 1 mM $CaCl_2$, 1 mM $MgCl_2$. α4β1 was eluted with 10 mM sodium acetate, pH 3.2, 0.1% Triton X-100, 1 mM $CaCl_2$, 1 mM $MgCl_2$ and immediately neutralized with HEPES buffer, pH 8.0. Fractions were assayed for α4β1 in a sandwich ELISA and for total protein using the BCA microprotein assay from Pierce. Peak fractions were pooled, aliquoted, and stored at −70 °C. Mab B5G10 (*41*) was purified from mouse ascites on Protein A Sepharose (Pharmacia).

*Assessing α4β1 Function.* Ninety-six-well Linbro plates were treated overnight at 4 °C with 10 μg/mL B5G10 (50 μL/well) in 50 mM $NaHCO_3$, pH 9.5. The plates were blocked with 2% Carnation nonfat dry milk in 10 mM Tris-HCl, pH 7.5, 150 mM NaCl (TBS) and washed 4 times with TBS complete (TBS, 0.1% BSA, 2 mM glucose, 10 mM Hepes, pH 7.5) plus 1 mM $CaCl_2$, 1 mM $MgCl_2$, 1 mM $MnCl_2$, 0.05% Tween-20. The plates were then treated for 1 h at 23 °C with serial 2-fold dilutions of purified α4β1 or α4β1-containing fractions, washed, and treated for 1 h at 23 °C with 50 μL/well of 0.75 μg/mL of a VCAM-Ig−alkaline phosphatase (AP) conjugate in the wash buffer, and washed and treated for 30 min at room temperature with 50 μL/well of the AP chromogenic substrate 4-nitrophenyl phosphate (10 mg/mL) in 10 mM glycine, pH 10.5, 1 mM $ZnCl_2$, 1 mM $MgCl_2$. Finally, 100 μL/well 3 N NaOH was added, and the absorbance was measured at 405 nm in a Molecular Devices microplate reader. Specific details about the assay are described elsewhere (L. Chen, R. B. Pepinsky, and R. R. Lobb, manuscript in preparation). Details describing the production and properties of the VCAM-Ig−AP conjugate and its use as a method for quantifying α4β1 on cells were previously described (*42*). α4β7 was purified from JY cells on B5G10 Sepharose following the protocol developed for α4β1 and was shown to be active in the VCAM-Ig−AP direct binding assay described above.

*Cross-Linking Studies with BIO-1494.* A modified form of BIO-1211 was synthesized for cross-linking studies where leucine was replaced with the 6-aminohexanoylamide of lysine (ahK). This variant of BIO-1211 was designated BIO-1494:

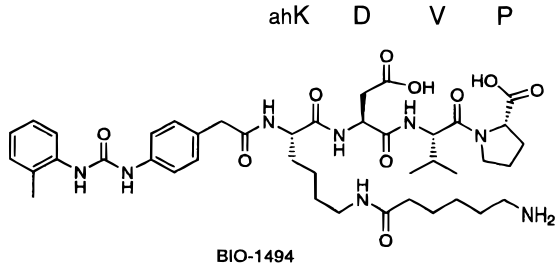


BIO-1494 was similar in potency to BIO-1211 when tested on α4β1 but contained a free amine that could be used to target cross-linking. BIO-1494 competed with BIO-1211 for the same binding pocket on α4β1 as evidenced by competition studies. Two different strategies were used for cross-linking BIO-1494 to α4β1. First, BIO-1494 was modified with the heterobifunctional photoactivated cross-linker *N*-5-azido-2-nitrobenzoyloxysuccinimide (ANB-NOS), and this reagent was used for cross-linking. Briefly, BIO-1494 (9 mM) in DMSO was treated with a 2-fold excess of ANB-NOS for 1 h at ambient temperature in the dark. The extent of modification of BIO-1494 was monitored by mass spectrometry. Under these conditions, most of the BIO-1494 was modified. The ANB-NOS-modified BIO-1494 was aliquoted and stored at −20 °C for subsequent use. Typically, purified α4β1 or α4β1 positive cells were treated with the activated conjugate within a range of 0.1−1 μM for 1 h at room temperature. Samples were then irradiated with 365 nm UV light from a long-wavelength mineral light for 10 min at room temperature, treated with electrophoresis sample buffer, and subjected to SDS−PAGE. Proteins that were cross-linked to BIO-1494 were visualized by Western blotting using a rabbit polyclonal antiserum that was raised against a BIO-1494−ovalbumin immunogen. The anti-BIO-1494 antibody was purified on Protein A Sepharose (Pharmacia). The second cross-linking strategy used the amino-

specific homobifunctional cross-linker disuccinimidyl suberate (DSS) or its water-soluble analogue bissulfosuccinimidyl suberate ($BS^3$). In these instances, α4β1 was first treated with BIO-1494 for 1 h at room temperature and then treated with 5 mM DSS (or 1 mM $BS^3$) for 1 h at room temperature. Samples were analyzed for cross-linking as described above. ANB-NOS, DSS, and $BS^3$ were obtained from Pierce.

*Preparation and Characterization of an Anti-BIO-1494-Specific Polyclonal Antiserum.* BIO-1494 was directly conjugated to ovalbumin using carbohydrate-targeted cross-linking chemistry (*34*) as follows. Ovalbumin (10 mg/mL in 100 mM sodium acetate, pH 5.0) was treated with 1.5 mM sodium periodate at room temperature for 40 min. The sample was desalted on a P6DG column (Bio-Rad) that had been equilibrated in 10 mM sodium acetate, 100 mM NaCl, pH 5.0. The periodate-activated ovalbumin was mixed with BIO-1494 and incubated overnight at room temperature. The reaction contained 6 mg/mL ovalbumin, 6 mg/mL BIO-1494, 1.4 mM sodium cyanoborohydride, 10% dimethylformamide, 50 mM MES, pH 6.5, and 100 mM NaCl. The sample was dialyzed into PBS. Four hundred micrograms of the conjugate was emulsified with Freund's complete adjuvant and immunized in rabbits using the lymph node immunization method. The resulting antisera were titered by ELISA on a BIO-1494−keyhole limpet hemocyanin (KLH) conjugate that had been prepared by first reacting BIO-1494 with Traut's reagent (Pierce) at a molar ratio of 1:2 and then treating this with maleimide-activated KLH (Pierce) at a molar ratio of 10:1 following methods provided by the manufacturer. Titers of 1:100 000 or greater were obtained. The ELISA signal was ablated if the antiserum was pretreated with BIO-1494, but was not affected after pretreatment with benzene-LDVP, indicating the 4-[(*N*′-2-methylphenyl)ureido]-phenylacetyl group was the primary epitope recognized by the antibody. The anti-BIO-1494 antisera showed no reactivity when tested on cells by FACS analysis or on cell lysates by Western blot analysis, but demonstrated a specific reactivity for α4β1 that had been treated with BIO-1494 in the presence of cross-linkers, which could be detected by Western blotting (see below). No reactivity was seen by FACS even after treatment with BIO-1494.

*Production of Epitope-Specific Anti-α4β1 Polyclonal Antisera.* A series of 18 peptides from the human β1 sequence, each 12−15 amino acids in length, were synthesized by Research Genetics, Inc. (Huntsville, AL). The peptides were designed to contain a single Cys residue for conjugation based either on the presence of an existing cysteine or on the addition of a Gly-Cys linker at the C-terminus of the peptide. Immunogens were generated by reacting each peptide with keyhole limpet hemocyanin (KLH) that had been activated for Cys cross-linking with maleimide groups (Pierce). Two milligrams of peptide was treated with 2 mg of KLH-maleimide in 400 μL of 100 mM HEPES, pH 7.5, for 30 min at 23 °C; 400 μg of the peptide−KLH complex was emulsified with Freund's complete adjuvant and immunized in rabbits using the lymph node immunization method. Each peptide was also conjugated to Sulfo-link activated resin from Pierce at 4 mg of peptide/mL of resin and used an affinity matrix for purifying the anti-peptide antibodies. Two hundred microliters of resin was treated with 3 mL of serum and washed with 50 mM Tris, pH 7.5, 150 mM NaCl, and the peptide-specific IgG was eluted with 50 mM glycine, pH 2.2, 250 mM NaCl and immediately neutralized with HEPES. Typically, we recovered approximately 200 μg of antibody per milliliter of immune antiserum. All of the antisera were screened by ELISA on the appropriate immunogen, and titers of 1:30 000 were routinely observed. The purified antibodies were also screened by SDS−PAGE/Western blotting on crude α4-K562 cell lysates, and from this analysis eight were chosen for peptide mapping studies based on their ability to selectively detect the β1 chain of α4β1. These epitope-specific antibody probes correspond to residues 1−13, QTDENRCLKANAK; residues 42−55, SARCDDLEALKKGC; residues 79−90, SKGTAEKLKPEGC; residues 136−147, KDDLENVKSLGTGC; residues 207−218, NKGEVFNELVGKGC; residues 219−231, QRISGNLDSPEGGC; residues 415−427, CPKKDSDSFKIRP; and residues 651−662, TKVESRDKLPQPGC. For two of the antibody probes, the peptide sequences were from the same CNBr fragment as another probe, and when analyzed by peptide mapping yielded identical profiles. In those instances, data from only one of the two are presented.

*Analysis of β1 Cleavage Products by CNBr Mapping.* α4β1 (10 μg/lane) was subjected to SDS−PAGE in a precast 10−20% gradient gel (Daiichi). Relevant bands were identified by $Zn^{2+}$ staining (*43*). Gel slices (2 × 1.5 × 1 mm) containing 2 μg of the β1 chain were excised with a razor blade and incubated at 23 °C for 1 h with 7 or 70 mg/mL CNBr in 0.1 N HCl, 0.1% 2-mercaptoethanol. CNBr-treated gel slices were washed twice for 5 min each with 25 mM Tris-HCl, pH 6.8, rinsed once with water, and incubated for 10 min at 37 °C with electrophoresis sample buffer (*44*). Gel slices were loaded onto a 10−20% gradient SDS−polyacrylamide gel, and the cleavage products were subjected to SDS−PAGE using a Tricine-based buffer system (*45*). The cleavage products were then transferred to nitrocellulose using the CAPS buffer system (*46*). Entire lanes each containing a β1 CNBr digest were excised from the blot and processed individually. The blots were blocked for 1 h at ambient temperature with 2% Carnation nonfat dry milk, in 10 mM Tris-HCl, pH 7.5, 150 mM NaCl (TBS), treated for 12 h with each of the primary antibodies specified in the block buffer, washed with TBS plus 0.05% Tween-20, incubated for 1 h at ambient temperature with the goat anti-rabbit−horseradish peroxidase conjugate in block buffer, washed with TBS plus 0.05% Tween-20, and developed with the ECL development system from Amersham.

## RESULTS

*Purification and Analysis of α4β1.* Integrin α4β1 was purified from α4-transfected K562 cells by immunoaffinity chromatography on a B5G10-Sepharose column. The protein was eluted in acidic buffer containing 0.1% Triton X-100 using a similar strategy used for purification on a Mab13 resin (*17*). Both B5G10 and Mab13 resins were tested and displayed similar yields, but contamination of α5β1 in the Mab13 product made B5G10 the preferred strategy. Figure 1 shows a silver-stained SDS−PAGE profile of the B5G10-purified product. Three prominent bands with masses of 155, 80, and 70 kDa were observed, corresponding to the β1 chain, the N-terminal fragment of the α4 chain, and the α4 C-terminal fragment. Six hundred micrograms of α4β1 was recovered from a 10 L culture of the α4-transfected K562

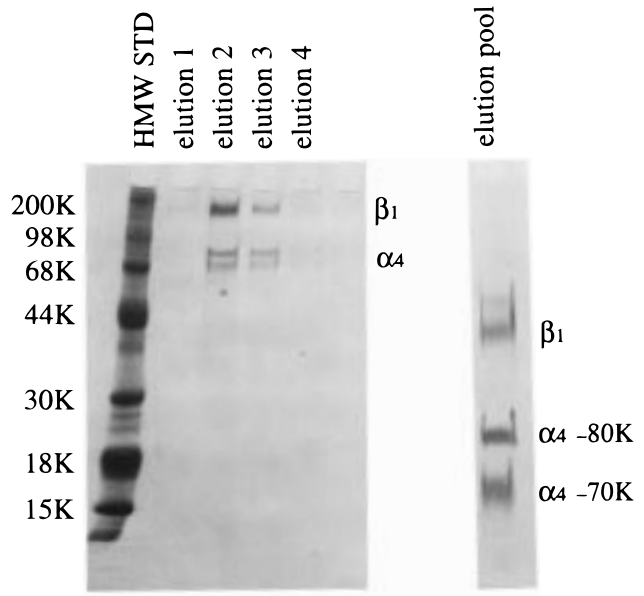


FIGURE 1: Purification of α4β1. Integrin α4β1 was purified from α4-transfected K562 cells by B5G10-Sepharose immunoaffinity chromatography. Column fractions were subjected to SDS−PAGE and visualized by silver staining. Individual elution fractions were analyzed on a 10−20% gradient gel (left panel) or as a pool on a 4−20% gel (right panel). Apparent masses for prestained high molecular mass protein standards (HMW STD) are indicated at the left.

cells. The overall yield was 40% based on a functional readout for α4β1. Batch to batch yields varied from 30 to 50%. α4β1 function was analyzed in an ELISA-type format where the α4β1 was captured on Mab B5G10 coated ELISA plates and then quantified using a VCAM-Ig reporter system.

Two other affinity-based purification strategies were also evaluated in which immobilized VCAM-Ig and BIO-1494 were used as functional ligands (data not shown). In these studies, binding was performed in the presence of $Ca^{2+}$, $Mg^{2+}$, and $Mn^{2+}$, and then the captured product was eluted with EDTA. Both methods generated functional α4β1 that was indistinguishable from protein generated on B5G10-Sepharose; however, the ligand-based purification strategies were highly inefficient with overall yields of less than 5%. For unknown reasons, most of the α4β1 failed to bind to the ligand supports.

*Specific Cross-Linking of α4β1 Small Inhibitor to the β1 Chain of α4β1.* Recently, a series of small molecule inhibitors of α4β1 (α4β1sm) were generated through synthetic chemistry with high affinity for α4β1 in cell-based assays measuring α4β1 function (K. C. Lin, R. R. Lobb, and S. P. Adams, unpublished experiments). The α4β1sm designated BIO-1211, a 70 pM α4β1 inhibitor, was highly efficacious in a sheep model of asthma, a model previously used to measure α4β1 function. To further characterize the binding properties of BIO-1211 and to localize the binding pocket on α4β1, we selected a chemical cross-linking strategy. A modified form of BIO-1211 designated BIO-1494 was generated for the cross-linking studies where Leu was replaced by Lys with 6-aminohexanoic acid attached to its ϵ-amino group. BIO-1494 was similar to BIO-1211 in potency but contained a free amine that could be used to target cross-linking (not shown). BIO-1494 and BIO-1211 effectively competed with VCAM-Ig-AP for α4β1 binding in the direct binding assay and with CS-1 for binding in the standard adhesion assay (data not shown).

Cross-linking with BIO-1494 was assessed both with the purified α4β1 and with the α4-transfected K562 cells used for α4β1 purification. In these studies, BIO-1494 was first modified through the free amino group on the hexylamine moiety with the photoactivated cross-linker ANB-NOS. The BIO-1494 ANB-NOS adduct was then incubated with α4β1 and activated with UV light. Cross-linking was assessed by SDS−PAGE/Western blotting, using an anti-BIO-1494 antibody to detect BIO-1494-containing complexes. Figure 2 shows results from a study where purified α4β1 was treated with BIO-1494 ANB-NOS. Under these conditions, a single band with molecular mass of 150 kDa was observed, which corresponds to the α4β1 β1 chain (Figure 2, lane a). Specific

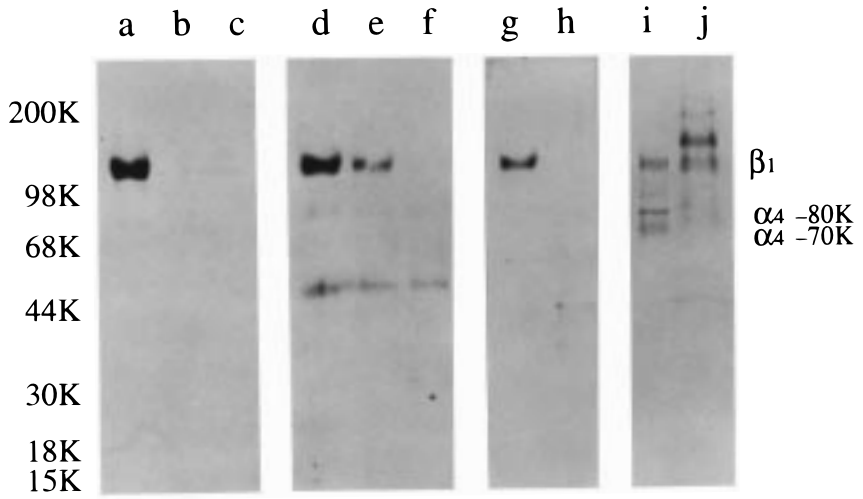


FIGURE 2: Site-specific cross-linking of purified α4β1 with BIO-1494 ANB-NOS. B5G10-purified α4β1 (lanes a−g) or α4β7 (lane h) that had been treated with BIO-1494 ANB-NOS was exposed to UV light and analyzed by SDS−PAGE/Western blotting using the anti-BIO-1494 antibody to detect cross-linking. All samples were incubated under standard $Mg^{2+}/Ca^{2+}$ conditions as described under Experimental Procedures. Samples in lanes b and c were treated with 0.1 μM BIO-1494 ANB-NOS plus 0.4 μM BIO-1211 or 4 μM BIO-1211. Samples in lanes e and f were treated under the standard conditions but with added $Mn^{2+}$ (2 mM) or EDTA (4 mM). Molecular masses at the left mark the positions of prestained molecular mass markers. The positions of the β1 and α4 chains are indicated at the right. Lanes i and j show silver-stained SDS−PAGE profiles of the purified α4β1 and α4β7, respectively.

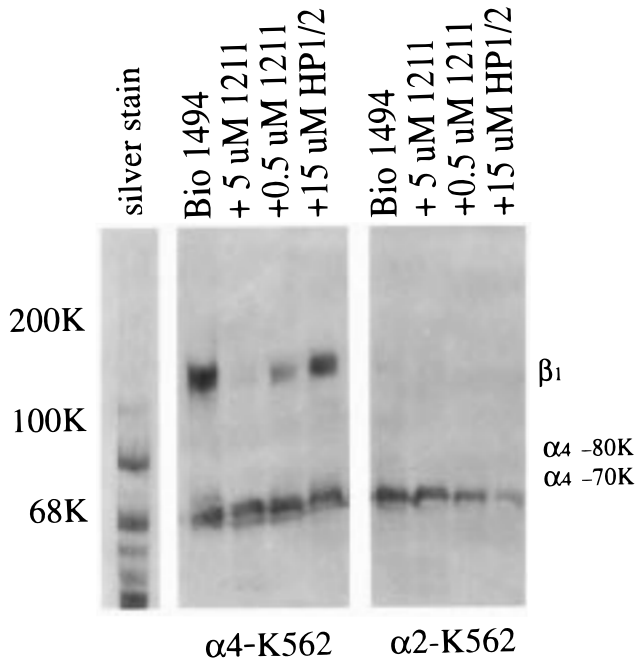


FIGURE 3: Analysis of BIO-1494/α4β1 complexes in BIO-1494 ANB-NOS treated cells. K562 cells transfected with the α4 or α2 chain were treated with BIO-1494 ANB-NOS and analyzed by SDS−PAGE/Western blotting with anti-BIO-1494 antisera. Cells were treated with BIO-1494 ANB-NOS either alone or in the presence of BIO-1211 or HP1/2 as indicated. The silver-stained profile on the left is from a parallel lane from the gel containing α4−K562 cell lysate. The positions of molecular mass standards are indicated at the left of the panel.

cross-linking to the β1 chain was observed over a wide range of BIO-1494 ANB-NOS concentrations (data not shown). BIO-1211 effectively competed with the BIO-1494 ANB-NOS for its ability to be cross-linked to α4β1, supporting the specificity of the reaction (Figure 2, lanes b and c). Peptide mapping studies discussed below revealed that cross-linking occurred at a single site. No signal was detected when α4β7 was subjected to the same cross-linking strategy (Figure 2, lane h), consistent with the lack of inhibitory activity of BIO-1211 toward α4β7, or when EDTA was added to the reaction cocktail (Figure 2, lane f).

Similar results were obtained when α4β1-expressing K562 cells were subjected to cross-linking with BIO-1494 ANB-NOS and analyzed by SDS−PAGE/Western blotting (see Figure 3). Again in the whole cell lysate, the 150 kDa band β1 chain of α4β1 was specifically labeled with BIO-1494, and the cross-linking was blocked with excess BIO-1211. The 150 kDa band was not detected when K562 cells transfected with the α2 chain of α2β1 (VLA2) were analyzed. The inability to label α2β1 with BIO-1494 under the same conditions that α4β1 is targeted indicates that the BIO-1494 binding pocket on α4β1 is dependent on the presence of both the α4 and β1 chains. The 65 kDa band present in the analysis from cell lysates was observed without BIO-1494 ANB-NOS treatment and therefore appears to be an artifact of the ECL detection system. We did not attempt to eliminate the band since it did not interfere with the analyses. BIO-1494/β1 chain cross-linking was not blocked by the anti-α4 neutralizing Mab HP1/2 (see Figure 3) despite the fact that HP1/2 is a competitive inhibitor of VCAM binding (*42*). This result was later verified in an independent binding study in which radioactive BIO-1211 was used as a probe for competitive binding (data not shown). Binding of the radioactive BIO-1211 to α4β1 was effectively competed for by VCAM and CS1 at concentrations that are consistent with their known binding constants, while HP1/2 treatment had no effect on BIO-1211 binding. Since a significant difference between the small molecule and the natural ligands is size, we infer that HP1/2 blocks binding through steric effects and not through direct binding at the ligand binding pocket.

*Localization of the BIO-1494 Binding Site by CNBr Mapping*. The BIO-1494 binding site was localized within the β1 sequence by using cross-linking to tag specific amino acids in direct contact with BIO-1494 and then subjecting the cross-linked complexes to CNBr mapping (*44, 47*). In these studies, α4β1 was treated with BIO-1494 ANB-NOS and subjected to SDS−PAGE. Gel slices containing the BIO-1494−β1 chain complex were incubated with CNBr, and then subjected to a second separation by SDS−PAGE, using Western blotting to analyze the cleavage products. CNBr cleaves proteins specifically at methionine residues. Since methionine residues are relatively rare, on average occurring 1 in every 50 amino acids, the resulting cleavage fragments can be analyzed by SDS−PAGE. Like most mapping strategies, CNBr mapping is based on the fact that each CNBr fragment from a protein can be represented by a subset of cleavage fragments and that once the pattern of cleavage fragments is known one simply has to match an unknown profile to the fragment-specific profiles. While many methods can be used to unravel fragmentation patterns (see *47, 48* for references), we selected epitope-specific antibodies to develop the map for the β1 chain.

The β1 chain sequence has 14 methionines and therefore was expected to produce a complex pattern of CNBr fragments under limiting cleavage conditions. Figure 4 shows CNBr digests of the BIO-1494−β1 chain complex where the anti-BIO-1494 antibody was used to visualize β1 containing the BIO-1494 moiety. With 7 mg/mL CNBr (lane b), approximately a dozen bands were observed with sizes ranging from 4 to 150 kDa. With harsher cleavage conditions (lanes c and d), the higher mass cleavage products were replaced by a series of fragments with masses of 12, 14, and 16 kDa. Interestingly, with increasing concentrations of CNBr, there was no buildup of a major cleavage product and there was a dramatic loss of the signal detected by the anti-BIO-1494 antibody. These observations suggested that the label was attached to a small cleavage product which was lost during the analysis. The smallest cleavage product observed, with apparent mass of 4 kDa, formed but then disappeared after prolonged treatment with CNBr (compare lanes c and d). The β1 sequence contained two regions where a series of low mass fragments could be generated, residues 130−173 (with three internal methionines) and residues 695−778 (with two internal methionines). Based on the relative size differences of cleavage products, in particular for the 12, 14, and 16 kDa fragments, we hypothesized that the linkage was in the region of small fragments spanning residues 130−173. This result was latter borne out in the fragment linkage maps discussed below. In digests with CNBr, most of the observed cleavage products are partials containing internal Met residues. While the cleavage profile is simplified after treatment with higher concentrations of CNBr, it is virtually impossible to drive

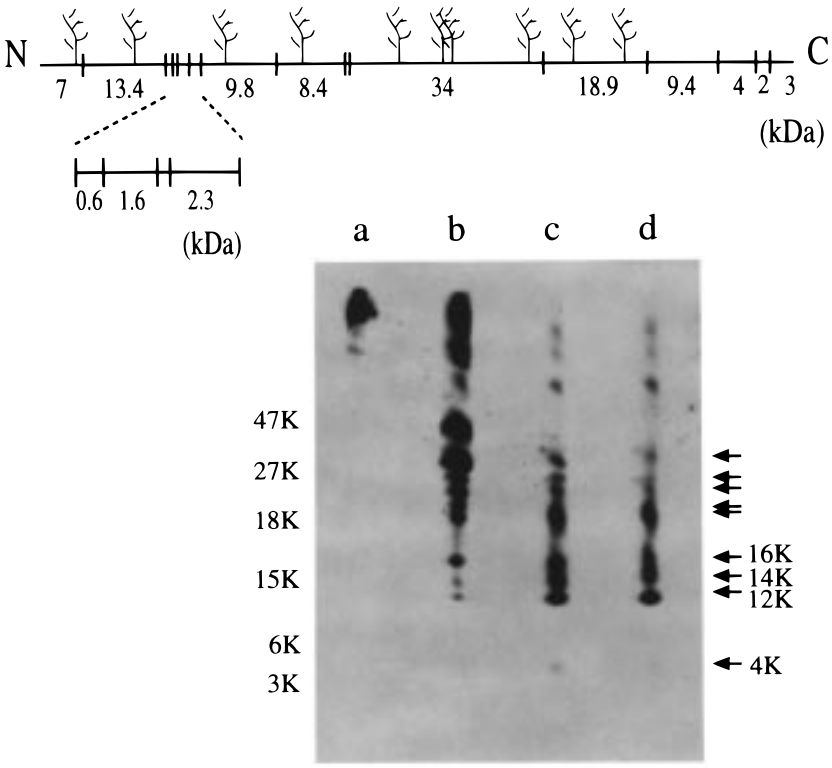


FIGURE 4: Analysis of the BIO-1494/$\beta$1 chain cross-linked complex by CNBr mapping. Gel slices containing the BIO-1494/$\beta$1 chain complex were incubated with CNBr and subjected to SDS−PAGE on a 10−20% gradient gel using the Tricine buffer system. Cross-linked cleavage products were detected by Western blotting with the anti-BIO-1494 antisera. Lane a, 0 mg/mL CNBr; lane b, 7 mg/mL CNBr, 1 h; lane c, 70 mg/mL CNBr, 1 h; lane d, 70 mg/mL CNBr, 16 h. The positions of molecular mass standards are indicated at the left. Arrowheads mark the CNBr fragments discussed in subsequent analysis. The schematic at the top marks the positions of Met residues (⊥) within the $\beta$1 chain sequence. Potential glycosylation sites are marked by tree-like structures. Theoretical masses indicated include an additional 3 kDa per glycosylation site. The expanded region at the base of the schematic corresponds to the 4 kDa fragment that was later identified as the site of cross-linking.

the cleavage reaction with CNBr to completion since oxidized Met residues, which are always present at varying levels, are resistant to cleavage.

To characterize the CNBr cleavage products from the $\beta$1 chain, we developed a series of sequence-specific peptide antisera that each could be used as a probe for one of the CNBr fragments. In this manner, fragmentation profiles representing individual CNBr fragments were identified. Results from these analyses are shown in Figure 5B. The six antibody probes tested are marked a−f. The locations of the peptides in the $\beta$1 sequence are indicated in Figure 5A. Each antibody was tested on $\beta$1 digests that were prepared at low and high CNBr concentrations. Numbers 1−13 denote the 13 possible CNBr fragments from the $\beta$1 subunit where 1 is the N-terminal fragment and 13 is the C-terminal fragment. As expected, each of the sets of profiles is unique and is characteristic of the CNBr fragment it represents. While only 6 of the 13 possible CNBr fragments were analyzed, the others could be readily inferred from the characterized maps, since each profile is simply an extension of that from the adjacent CNBr fragment(s).

When the cleavage profiles detected with the anti-BIO-1494 antibody (marked with an asterisk in Figure 5B) were compared with those from the anti-peptide antibodies, we observed a striking similarity with profiles b and c. In particular, the series of fragments with masses of 12, 14, and 16 kDa are readily apparent. In contrast, CNBr profiles d and f, representing the two other possible candidates for the cross-linking, are clearly distinct. Thus, the epitope mapping data support our original prediction. The b and c like features of the BIO-1494 profile localize the cross-link site within CNBr fragments 2−4. Of these possibilities, the presence of the 4 kDa intermediate in the BIO-1494 digest rules out CNBr fragment 2 as the target since CNBr fragment 2 itself is 12 kDa. Similarly, the presence of the 12 kDa fragment in the BIO-1494 digest rules out CNBr 4 since it is absent from the profile derived from CNBr fragment 4 (profile c). The most likely explanation for the result with BIO-1494 was that CNBr fragment 3 was the target sequence.

To test this notion, we reasoned that if CNBr fragment 3 were the target of the BIO-1494 ANB-NOS cross-link and we changed the cross-linker to one that could not target CNBr fragment 3, then a different cleavage pattern might be generated. Indeed, the results from cross-linking with DSS supported this notion. When $\alpha$4$\beta$1 was treated with BIO-1494 and subjected to cross-linking with DSS, we obtained the results shown in Figure 6, lanes b and c. As with BIO-1494 ANB-NOS, the $\beta$1 chain was tagged with BIO-1494 and cross-linking could be blocked with excess BIO-1211 (Figure 6, lanes d and e) or by treatment with EDTA (lane f). When the $\beta$1 chain/BIO-1494 DSS complex was subjected to CNBr mapping, we obtained the results shown in Figure 7. The cleavage data with 7 mg/mL CNBr (lane c) were indistinguishable from cleavage data from the ANB-NOS complex (lane a) whereas significant differences were apparent with 70 mg/mL CNBr (compare lanes b and d). The most significant change was the loss of the 12 kDa

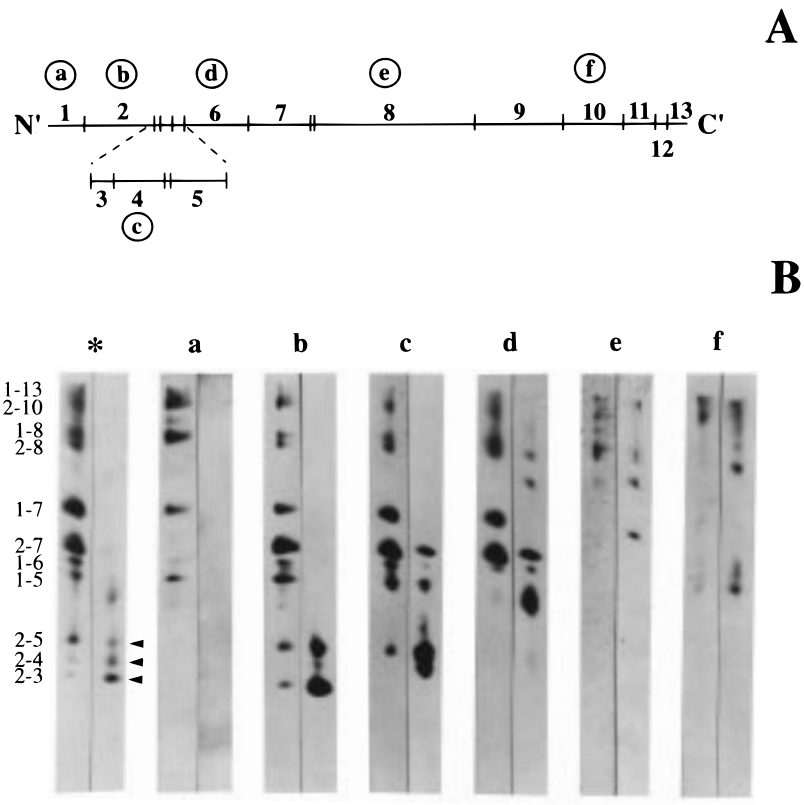


FIGURE 5: Identification of β1 CNBr fragments by epitope mapping. Antisera targeted at synthetic peptides in the β1 sequence were developed in rabbits and used to probe CNBr digests of the β1 chain by Western blotting. The relative positions of the peptides within the β1 sequence are indicated in panel A (marked a−f). Specific CNBr fragments are marked numerically where 1 denotes the N-terminal fragment and 13 denotes the C-terminal fragment. The actual peptide mapping data are presented in panel B using the same lettering scheme to denote specific peptide antisera. Each analysis was performed on digests prepared at 7 and 70 mg/mL CNBr. Data below the asterisk were generated with the anti-BIO-1494 antiserum. Designations at the left of the panel indicate relevant fragment compositions for the BIO-1494-containing CNBr fragments that were inferred from the mapping data. Arrowheads mark the positions of the 12, 14, and 16 kDa bands.

fragment. The absence of this spot indicates that the cross-link was indeed shifted off CNBr fragment 3 as predicted. The presence of the 14 and 16 kDa fragments indicates that the BIO-1494 DSS linkage is now associated with CNBr fragment 4. In this particular analysis, the low molecular weight CNBr fragments were run off the gel in order to obtain better resolution in the relevant region. Both the ANB-NOS and DSS profiles contain the 4 kDa CNBr fragment (data not shown).

In addition to the β1 chain, three other adducts were labeled with BIO-1494 as a result of DSS cross-linking: the 80 kDa fragment of the α4 chain and two high molecular weight complexes that resulted from protein−protein cross-links between the α and β chains (see Figure 6, lane b). These other species were also sensitive to BIO-1211 and EDTA treatment (Figure 6, lanes d−f), indicating that like the β1 chain linkage to BIO-1494, they were also specific. CNBr mapping data for the 80 kDa fragment of the α4 chain are shown in Figure 7, lanes e and f. Five prominent and one minor cleavage products were generated with masses of 30, 40, 45, 55, 70, and 76 kDa. Based on the apparent sizes and number of spots, we infer that the site of cross-linking is from within the N-terminal-most CNBr fragment (amino acid residues 40−219 in the α4 precursor sequence). Several observations support this notion. First, of the six possible CNBr fragments from this region of the α4 chain, only the N-terminal fragment is of the appropriate size. The other CNBr fragments are all less than 15 kDa in size and therefore would be expected to yield smaller labeled fragments. None of the 10−18 kDa CNBr fragments that are visible in the silver-stained profile of the digest were labeled with BIO-1494. Second, one can use the theoretical masses of the individual CNBr fragments to predict what the cleavage profile should look like if cross-linking had occurred within a given CNBr fragment and then compare these profiles to BIO-1494 data. The hypothetical pattern for the N-terminal fragment would have masses of 26, 39, 44, 55, 71, and 83 kDa, which correlates extremely well with the actual cleavage data. None of the other patterns resemble the observed data. Third, the 30 and 40 kDa bands were submitted to N-terminal sequencing, and a primary sequence corresponding to the N-terminus of the α4 chain was obtained. In both instances, multiple sequences were observed, limiting the usefulness of the sequence data. The CNBr cleavage profiles for the other bands (ca. 200 and 250 kDa) contained fragments that were readily interpretable as mixtures of both the α and β chain profiles together (data not shown). They thus represent cross-linked α/β chain protein−protein complexes in which the α and β chain components were cross-linked to BIO-1494.

DSS cross-linking was also performed on BIO-1494-treated α4-transfected K562 cells. As with the purified integrin, both the α4 and β1 chains were detected after DSS cross-linking (data not shown). However, the cell-associated α4β1 was particularly sensitive to protein−protein cross-linking, which complicated the analysis, and resulted in

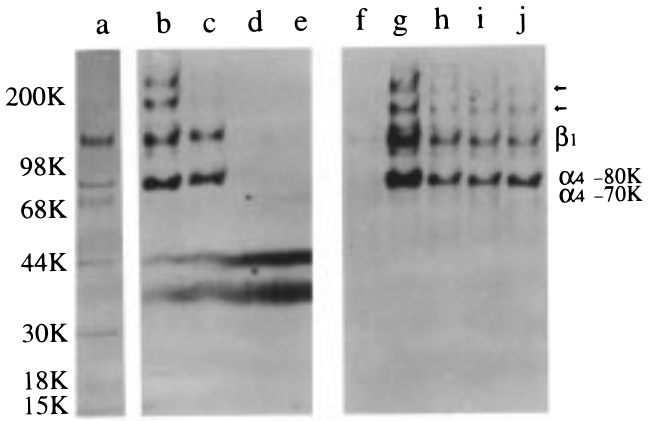


FIGURE 6: Site-specific cross-linking of BIO-1494/α4β1 complex with DSS. The ability of α4β1 to be cross-linked to BIO-1494 was also evaluated with DSS (lanes b−e) or its water-soluble analogue $BS^3$ (lanes f−k) using Western blotting with the anti-BIO-1494 antibody to detect cross-linking. B5G10-purified α4β1 was first incubated with BIO-1494 for 1 h at ambient temperature and then treated with the cross-linker for an additional 1 h. α4β1/BIO-1494 complexes were treated with 10 mM DSS (lane b), 5 mM DSS (lane c), or 5 mM DSS plus 5 μM or 0.5 μM BIO-1211 (lanes d and e). The effect of divalent ions on cross-linking is shown in lanes f−j. Lane f, 4 mM EDTA-treated sample. Lane g, $BS^3$ control under standard conditions. Lanes h−j, 2 mM $Mn^{2+}$-treated samples, where manganese was added simultaneously with BIO-1494, 30 min before BIO-1494 treatment or for 30 min after BIO-1494 treatment, respectively. Lane a, silver-stained profile of α4β1. Molecular masses at the left mark the positions of prestained standards.

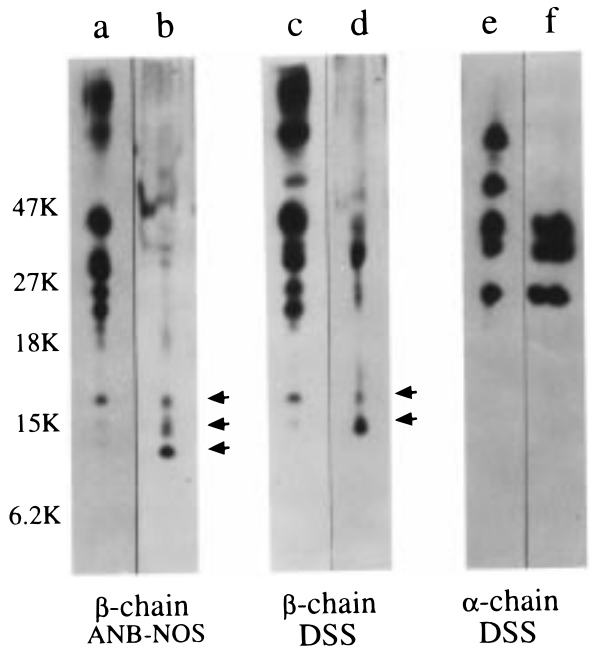


FIGURE 7: Analysis of DSS-cross-linked BIO-1494-containing complexes by CNBr mapping. BIO-1494/α4β1 complexes that had been generated with DSS were analyzed by CNBr mapping as described in Figure 5 for the ANB-NOS-linked complexes. Samples were analyzed after digestion for 1 h with 7 (lanes a, c, and e) and 70 mg/mL CNBr (lanes b, d, and f). Lanes a and b, BIO-1494/β1 chain complexes generated with ANB-NOS. Lanes c and d, BIO-1494/β1 chain complexes generated with DSS. Lanes e and f, BIO-1494/α4 chain complexes generated with DSS.

profiles that were highly variable from study to study. The same DSS concentrations that were useful for promoting cross-linking between α4β1 and BIO-1494 with the purified integrin caused the cell-associated α4β1 to form a complicated series of high molecular weight complexes that were uninterpretable.

Since α4β1 function is dependent on divalent ions, we tested the effects of $Ca^{2+}$ and $Mn^{2+}$ on its susceptibility to cross-linking with BIO-1494. As expected, EDTA treatment blocked our ability to cross-link BIO-1494 to purified α4β1 (see Figure 2, lane f, for results with ANB-NOS 1494, and Figure 6, lane f, for results with DSS) and cell-associated α4β1 (data not shown). Surprisingly, $Mn^{2+}$ treatment interfered with the extent of cross-linking, reducing the observed signal by 75%. Similar results were obtained with ANB-NOS and DSS treatments (see Figures 2 and 6) and occurred whether the $Mn^{2+}$ was added before, during, or after BIO-1494 treatment (Figure 6, lanes h−j). Since BIO-1211 exhibits approximately a 300-fold higher affinity for the $Mn^{2+}$-activated state of α4β1 treatment versus the nonactivated state (L. L. Chen and R. B. Pepinsky, unpublished experiments), we infer that the loss of signal is due to a change in conformation such that the α4β1/BIO-1494 complex is no longer susceptible to cross-linking.

## DISCUSSION

We have used chemical cross-linking to study the interactions between α4β1 and its ligands. Using a small molecule inhibitor based on the LDV sequence from CS1 fibronectin (BIO-1494), we specifically cross-linked the inhibitor to α4β1 on its β1 chain alone with ANB-NOS or on both the α4 and β1 chains with DSS. Several types of experiments were used to define the specificity of the cross-linking. First, cross-linking with BIO-1494 could be blocked with BIO-1211, a closely related analogue that is not susceptible to cross-linking. Second, cross-linking was dependent on the presence of divalent cations and could be completely blocked with EDTA, consistent with the known metal binding requirement of integrins. Third, BIO-1494 failed to be cross-linked to the functionally related integrin α4β7, that shares a common α chain, or to α2β1 (VLA2), which shares the same β chain. Finally, cross-linking specificity could be inferred from the localization studies performed by peptide mapping. A single site was identified with both cross-linkers tested. Cross-linking with BIO-1494 was performed both on purified α4β1 and on cell-associated α4β1 with similar success.

The site of the BIO-1494 ANB-NOS cross-link was localized to within the sequence DLSYSM (residues 130−136) by CNBr mapping. The lack of specificity of the azido group prevented further resolution. Previously, Kamata and co-workers generated a mutant form of α4β1 containing a D-130 to A point mutation (*20*). The ligand binding properties of the mutant form of α4β1 were almost totally blocked when tested with CS1 and greatly reduced with VCAM, supporting a role for this region of α4β1 in ligand binding. Others have speculated that the DLSYSM sequence is involved in metal binding (*26*, *49*). While we cannot distinguish between these possibilities, the cross-linking data clearly show that ligand binding occurs in this region. Interestingly, the addition of $Mn^{2+}$, a known activating signal for ligand binding (*8*), reduced the extent of cross-linking. Whether this result reflects a local perturbation in the α4β1 structure producing a conformation that is no longer sus-

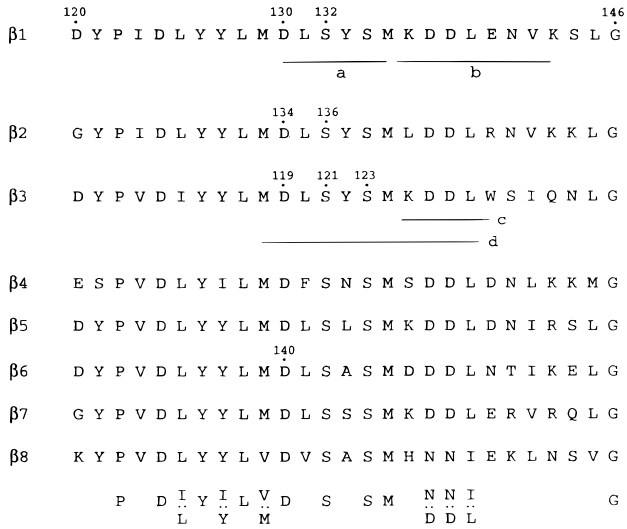


FIGURE 8: Alignment of conserved $\beta$ chain sequences in the region of cross-linking. Amino acid residues 120−146 in the human $\beta$1 sequence (*54*) and the corresponding sequences from human $\beta$2 through $\beta$8 are shown (see *55* for references). Significant sequences based on functional data are highlighted. Regions a and b in $\beta$1 denote the regions detected in this study by ANB-NOS and DSS cross-linking. D-130 and Ser-132 in the $\beta$1 sequence were identified by mutagenesis (*20*, *23*). Region c in the $\beta$3 sequence was identified by cross-linking and phage display technology (*25*, *27*). Region d was shown to be directly involved in cation and ligand binding in studies using a synthetic peptide derived from the sequence (*49*). D-119, S-121, and Ser-123 in $\beta$3 were identified by mutagenesis (*56*). D-134 and Ser-136 in the $\beta$2 sequence (*55*) and D-140 in the $\beta$6 sequence were identified by mutagenesis (*57*).

ceptible to cross-linking or reflects a direct effect of the metal on ligand binding remains to be determined. While the later possibility has been proposed for other integrins (*49*, *50*), we favor the former for α4β1, since $Mn^{2+}$ did not compete for small molecule binding when radioactive BIO-1211 was used to monitor binding (L. L. Chen and R. B. Pepinsky, unpublished experiments).

When DSS was used in place of ANB-NOS, the site of cross-linking was shifted to the adjacent sequence KD-DLENVK (residues 136−143). Since DSS only targets amino groups, we can infer that either K-136 or K-143 is tagged. Of these possibilities, K-136 is the more probable site of cross-linking. This notion is based on a structural model of the region that had been constructed with the framework defined by the crystal structure of the I-domain of integrin CR3; however, this hypothesis remains to be tested (Michael Karpusas, personal communication; see *28*, *51* for similar structural models). The minor differences in the proximity of the cross-link observed with ANB-NOS and DSS presumably reflect property differences of the cross-linkers themselves since ANB-NOS is a rigid structure with a 7.7 Å spacer arm and DSS has a flexible spacer arm with a span of 11.4 Å. The added flexibility of the DSS linkage presumably accounts for why the BIO-1494 DSS moiety also could become cross-linked with the α chain.

The mapping data for α4β1 were particularly rewarding in that they identified the same region in the $\beta$1 sequence that previously had been shown to be involved in ligand binding to the $\beta$3 chain of integrin αIIbβ3 (*27*) and αvβ3 (*52*, *53*). These data are summarized in Figure 8. In the αIIbβ3 studies, K-125 was targeted when an RGD-containing peptide ligand was used for cross-linking. K-125 in αIIbβ3 corresponds to K-136 in α4β1. In αvβ3, cross-linking was localized to within residues 61−203. This region overlaps with the region identified in αIIbβ3. Subsequent studies using phage display technology to investigate $\beta$3/ligand interactions identified the sequence DLLW (corresponding to residues 126−129 in the $\beta$3 sequence) as being involved in ligand binding (*25*). The striking similarity in the data we generated for α4β1 and the previous work with αIIbβ3 implies that the structure of the ligand binding pocket is highly conserved between the two integrins. Furthermore, the high degree of homology among the known $\beta$ chain sequences in this region suggests that this binding pocket will be a common structural feature of all integrins (see Figure 8). Further studies with other integrins will be necessary to test this hypothesis. In addition to the sequence homology among the $\beta$ chains, this region also shares structural homology with the I-domain found on certain α chains (*26*). For the $\beta$3 subunit, residues 211−231 (corresponding to residues 220−240 of the $\beta$1 sequence) have also been implicated in ligand binding based on the ability of synthetic peptides derived from this region to bind RGD-containing ligands and to block integrin αIIbβ3 binding to fibronectin. Recent mutagenesis studies with the $\beta$1 subunit support this notion (*23*). We saw no evidence for this interaction in our cross-linking analysis of α4β1 either with ANB-NOS or with DSS.

The DSS cross-linking studies also revealed that the α chain was in close proximity to the BIO-1494 binding site. In these studies, only the 80 kDa fragment was tagged with BIO-1494, indicating that the site of cross-linking is in the N-terminal half of the α chain. When the 80 kDa/BIO-1494 complex was digested with CNBr and analyzed by Western blotting for the presence of BIO-1494, a series of six bands were detected with masses of 30, 40, 45, 55, 70, and 76 kDa. While the α4 cleavage profile was not subjected to the extensive mapping analysis performed with the $\beta$1 chain, the cleavage data provide important clues as to the proximity of the cross-link. First, the 80 kDa fragment has only five internal methionines, and thus CNBr fragments with masses of 26, 13, 4, 11, 16, and 12 kDa should be generated, where 26 kDa is the N-terminal fragment and 12 kDa is the C-terminal fragment. The absence of the BIO-1494 tag in any of the 10−18 kDa CNBr fragments indicates that a 30 kDa fragment is the smallest one labeled. Second, one can predict what the cleavage profiles would look like based on the apparent masses of the six CNBr fragments. The pattern for the N-terminal fragment would have masses of 26, 39, 44, 55, 71, and 83 kDa, which correlates extremely well with the actual cleavage data. None of the other patterns resemble the observed data. Third, the 30 and 40 kDa bands were submitted to N-terminal sequencing, and a primary sequence corresponding to the N-terminus of the α4 chain was obtained. Together these observations suggest that BIO-1494 binding occurs within residues 1−180 of the α4 sequence. This notion is consistent with available data generated by epitope mapping of neutralizing antibodies for α4β1 and mutagenesis studies (*19*, *20*, *58*). The recently proposed $\beta$-propeller model for the α4 subunit structure (*58*, *59*) provides an interesting framework for designing future studies. Our ability to dissect Mab HP1/2 binding from ligand binding with BIO-1494 indicates that the small molecule probes are particularly well suited for this work.

To perform the cross-linking studies with α4β1, it was necessary to develop a method that yielded highly purified product that retained function. Four different purification strategies were tested using B5G10, Mab13, VCAM-Ig, or BIO-1494 as affinity steps. The VCAM-Ig and BIO-1494 strategies failed for unknown reasons. Both of the immunoaffinity steps were successful. α4β1 from the B5G10 purification was superior due to contamination of the Mab13-purified product by α5β1. The Mab13 product also contained a second form of the β1 chain with slightly lower molecular weight that was not observed after B5G10 purification. The B5G10 purification method was also applied successfully for the purification of α4β7 from JY cells. The purified α4β1 and α4β7 preparations both were functional in the VCAM-Ig binding assay.

The purified integrins were tested for activity in an ELISA-type format using VCAM-Ig−AP as a reporter system in a manner analogous to that previously used to assess functional α4β1 on cells (*42*). Two formats were developed: a direct binding assay where the integrins were coated onto ELISA plates and monitored with VCAM-Ig−AP and an indirect format where they were collected on B5G10-coated plates and monitored with VCAM-Ig. Details and applications of these assays are described elsewhere (L. Chen, B. Pepinsky, and R. Lobb, manuscript in preparation). The direct coating assay was particularly useful for studying structure−function since it takes less time to perform than the indirect assay and uses less protein. The assay was highly reproducible (typically, coating concentrations of 1−2 μg of integrin/mL were used). However, the assay was dependent on sample purity and was very sensitive to detergent levels in the integrin preparation. The indirect assay was extremely valuable for monitoring purification since it was largely independent of these variables.

The extensive mutagenesis studies and epitope mapping of functional antibodies have provided a model for the specific regions in integrins that are critical for function. Despite the abundance of genetic data, biochemical evidence for these interactions has been limited to studies of RGD integrins typified by $\alpha_{IIb}\beta 3$, largely because of the lack of appropriate probes for function for other classes of integrins. We have developed BIO-1494 as a novel probe for the LDV integrin α4β1. The cross-linking studies we performed with α4β1 support and expand upon these observations, and provide the first glimpse of the ligand binding site on an LDV integrin. The data revealed that both chains in α4β1 are in close proximity with the ligand and along with the previously published RGD integrin data suggest that the ligand binding pocket is a highly conserved structure among integrins. The CNBr peptide maps that were constructed with the β1 chain of α4β1 should be readily applicable to the other VLA integrins since they share a common β1 chain. Cross-linking provides a direct method for probing structure−function that to date has had limited use in studying integrin biology. The tools we developed for α4β1 should be particularly valuable for probing mechanisms leading to integrin activation/inactivation.

## ACKNOWLEDGMENT

We thank Konrad Miatkowski and Joe Amatucci for growing the JY and α4- and α2-transfected K562 cells, George Deegan for assisting in the preparation of rabbit antisera, and Diane Leone, Andrew Sprague, and William Delahunt for assisting in the functional analysis of the various inhibitors. We also thank Laurie Osborn for helpful discussions, Alphonse Galdes for critically reading the manuscript, and Martin Hemler for providing the K562 transfectants and the B5G10 hybridoma.

## REFERENCES

1. Wayner, E. A., Garcia-Pardo, A., Humphries, M. J., McDonald, J. A., and Carter, W. G. (1989) *J. Cell Biol. 109*, 1321−1330.
2. Guan, J. L., and Hynes, R. O. (1990) *Cell 60*, 53−61.
3. Elices, M. J., Osborn, L., Takada, Y., Crouse, C., Luhowskyj, S., Hemler, M. E., and Lobb, R. R. (1990) *Cell 60*, 577−584.
4. Lobb, R. R., and Hemler, M. E. (1994) *J. Clin. Invest. 94*, 1722−1728.
5. Springer, T. A. (1994) *Cell 76*, 301−314.
6. Chan, B. M. C., Wong, J. G. P., Rao, A., and Hemler, M. E. (1991) *J. Immunol. 147*, 398−404.
7. Shimizu, Y., VanSeventer, G. A., Horgan, K. J., and Shaw, S. (1990) *Nature 345*, 250−253.
8. Masumoto, A., and Hemler, M. E. (1993) *J. Biol. Chem. 268*, 228−234.
9. Clark, E. A., and Brugge, J. S. (1995) *Science 268*, 233−239.
10. Xiao, J., Messinger, Y., Jin, J., Myers, D. E., Bolen, J. B., and Uckun, F. M. (1996) *J. Biol. Chem. 271*, 7659−7664.
11. Yamada, K. M., and Miyamoto, S. (1995) *Curr. Opin. Cell Biol. 7*, 681−689.
12. Stewart, M., Thiel, M., and Hogg, N. (1995) *Curr. Opin. Cell Biol. 7*, 690−696.
13. Yednock, T. A., Cannon, C., Vandevert, C., Goldbach, E. G., Shaw, G., Ellis, D. K., Liaw, C., Fritz, L. C., and Tanner, L. I. (1995) *J. Biol. Chem. 270*, 28740−28750.
14. Bednarczyk, J. L., Szabo, M. C., and McIntyre, B. W. (1992) *J. Biol. Chem. 267*, 25274−25281.
15. Teixido, J., Parker, C., Kassner, P. D., and Hemler, M. E. (1992) *J. Biol. Chem. 267*, 1786−1791.
16. Blue, M.-L., Davis, G., Conrad, P., and Kelley, K. (1993) *Immunology 78*, 80−85.
17. Makarem, R., Newham, P., Askari, J. A., Green, L. J., Clements, J., Edwards, M., Humphries, M. J., and Mould, A. P. (1994) *J. Biol. Chem. 269*, 4005−4011.
18. Shih, D.-T., Edelman, J. M., Horwitz, A. F., Grunwald, G. B., and Buck, C. A. (1993) *J. Cell Biol. 122*, 1361−1371.
19. Schiffer, S. G., Hemler, M. E., Lobb, R. R., Tizard, R., and Osborn, L. (1995) *J. Biol. Chem. 270*, 14270−14273.
20. Kamata, T., Puzon, W., and Takada, Y. (1995) *Biochem. J. 305*, 945−951.
21. Luque, A., Gómez, M., Puzon, W., Takada, Y., Sánchez-Madrid, F., and Cabañas, C. (1996) *J. Biol. Chem. 271*, 11067−11075.
22. Irie, A., Kamata, T., Puzon-McLaughlin, W., and Takada, Y. (1995) *EMBO J. 14*, 5550−5556.
23. Puzon-McLaughlin, W., and Takada, Y. (1996) *J. Biol. Chem. 271*, 20438−20443.
24. Takada, Y., Elices, M. J., Crouse, C., and Hemler, M. E. (1989) *EMBO J. 8*, 1361−1368.
25. Pasqualini, R., Koivunen, E., and Ruoslahti, E. (1995) *J. Cell Biol. 130*, 1189−1196.
26. Lee, J.-O., Rieu, P., Arnaout, A., and Liddington, R. (1995) *Cell 80*, 631−638.
27. D'Souza, S. E., Ginsberg, M. H., Burke, T. A., Lam, S. C-T., and Plow, E. F. (1988) *Science 242*, 91−93.
28. Tozer, E. C., Liddington, R. C., Sutcliffe, M. J., Smeeton, A. H., and Loftus, J. C. (1996) *J. Biol. Chem. 271*, 21978−21984.
29. D'Souza, S. E., Ginsberg, M. H., Burke, T. A., and Plow, E. F. (1990) *J. Biol. Chem. 265*, 3440−3446.
30. Wayner, E. A., and Kovach, N. L. (1992) *J. Cell Biol. 116*, 489−497.
31. Lobb, R. R., Chi-Rosso, G., Leone, D., Rosa, M., Newman, B., Luhowshyj, S., Osborn, L., Schiffer, S., Benjamin, C., Dougas, I., Hession, C., and Chow, E. P. (1991) *Biochem. Biophys. Res. Commun. 178*, 1498−1504.

32. Pepinsky, B., Hession, C., Chen, L. L., Moy, P., Burkley, L., Jakobowski, A., Chow, E. P., Chi-Rosso, G., Luhowshyj, S., and Lobb, R. (1992) *J. Biol. Chem. 267*, 17820−17826.
33. Dustin, M. L., Olive, D., and Springer, T. A. (1989) *J. Exp. Med. 169*, 503−517.
34. Pepinsky, R. B., Chen, L. L., Meier, W., and Wallner, B. P. (1991) *J. Biol. Chem. 266*, 18244−18249.
35. Jakubowski, A., Rosa, M. D., Bixler, S., Lobb, R., and Burkley, L. C. (1995) *Cell Adhes. Commun. 3*, 131−142.
36. Wang, J.-H., Pepinsky, B., Stehle, T., Liu, J.-H., Karpusas, M., Browning, B., and Osborn, L. (1995) *Proc. Natl. Acad. Sci. U.S.A. 92*, 5714−5718.
37. Jones, E. Y., Davis, S. J., Williams, A. F., Harlos, K., and Stuart, D. I. (1992) *Nature 360*, 232−239.
38. Vanderslice, P., Ren, K., Revelle, J. K., Kim, D. C., Scott, D., Bjercke, R. J., Yeh, E. T. H., Beck, P. J., and Kogan, T. P. (1997) *J. Immunol. 158*, 1710−1718.
39. Jackson, D. Y., Quan, C., Artis, D. R., Rawson, T., Blackburn, B., Struble, M., Fitzgerald, Chui, H., Renz, M., Jones, S., and Fong, S. (1997) *J. Med. Chem. 40*, 3359−3368.
40. Abraham, W. M., Ahmed, A., Sielczak, M. W., Narita, M., Arrhenius, T., and Elices, M. J. (1997) *Am. J. Respir. Crit. Care Med. 156*, 696−703.
41. Hemler, M. E., Huang, C., Takada, Y., Schwarz, L., Strominger, J. L., and Clabby, M. L. (1987) *J. Biol. Chem. 262*, 11478−11485.
42. Lobb, R. R., Antognetti, G., Pepinsky, R. B., Burkley, L., Leone, D., and Whitty, A. (1995) *Cell Adhes. Commun. 3*, 385−397.
43. Fernandez-Patron, C., Calero, M., Collazo, P. R., Garcia, J. R., Madrazo, J., Musacchio, A., Soriano, F., Estrada, R., Frank, R., Castellanos-Serra, L. R., and Mendez, E. (1995) *Anal. Biochem. 224*, 203−211.
44. Pepinsky, R. B. (1983) *J. Biol. Chem. 258*, 11229−11235.
45. Schägger, H., and von Jagow, G. (1987) *Anal. Biochem. 166*, 368−379.
46. Matsudaira, P. (1987) *J. Biol. Chem. 262*, 10035−10038.
47. Pepinsky, R. B. (1991) *Methods Enzymol. 198*, 260−272.
48. Pepinsky, R. B., Papayannopoulos, I. A., Krishna, N. K., Craven, R. C., Chow, E. P., and Vogt, V. M. (1995) *J. Virol. 69*, 6430−6438.
49. D'Souza, S. E., Haas, T. A., Piotrowics, R. S., Byers-Ward, V., McGrath, D. E., Soule, H. R., Cierniewski, C., Plow, E. F., and Smith, J. W. (1994) *Cell 79*, 659−667.
50. Qu, A., and Leahy, D. J. (1996) *Structure 4*, 931−942.
51. Tuckwell, D. S., and Humphries, M. J. (1997) *FEBS Lett. 400*, 297−303.
52. Smith, J. W., and Cheresh, D. A. (1988) *J. Biol. Chem. 263*, 18726−18731.
53. Lin, E. C. K., Ratnikov, B. I., Tsai, P. M., Carron, C. P., Myers, D. M., Barbas, C. F., and Smith, J. W. (1997) *J. Biol. Chem. 272*, 23912−23920.
54. Argraves, W. S., Suzuki, S., Arai, H., Thompson, K., Pierschbacher, M. D., and Ruoslahti, E. (1987) *J. Cell Biol. 105*, 1183−1190.
55. Bajt, M. L., Goodman, T., and MacGuire, S. L. (1995) *J. Biol. Chem. 270*, 94−98.
56. Bajt, M. L., and Loftus, J. C. (1994) *J. Biol. Chem. 269*, 20913−20919.
57. Huang, X.-Z., Chen, A., Agrez, M., and Sheppard, D. (1993) *Mol. Biol. Cell. 4*, 283a.
58. Irie, A., Kamata, T., and Takada, Y. (1997) *Proc. Natl. Acad. Sci. U.S.A. 94*, 7198−7203.
59. Springer, T. A. (1997) *Proc. Natl. Acad. Sci. U.S.A. 94*, 65−72.

BI980311A